Volume 22, issue 3 June 2012
ISSN 0959-440X

Current Opinion in Structural Biology

Tom L Blundell & Keith Moffat, Editors

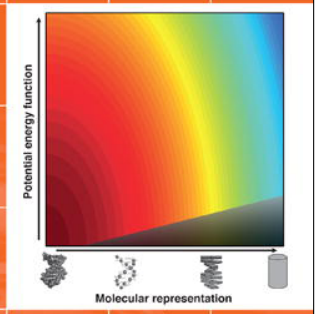

June 2012

Nucleic acids

Edited by Joseph D Puglisi and James R Williamson

Sequences and topology

Edited by Christine A Orengo and James Whisstock

August 2012 Engineeering and design • Membranes
October 2012 Carbohydrates and glycoconjugates • Biophysical methods
December 2012 Catalysis and regulation • Proteins
February 2013 Folding and binding • Protein-nucleic acid interactions
April 2013 Theory and simulation • Macromolecular assemblies

CURRENT OPINION

Available online at www.sciencedirect.com

SciVerse ScienceDirect

Current Opinion in Structural Biology

Cations in charge: magnesium ions in RNA folding and catalysis

Jessica C Bowman, Timothy K Lenz, Nicholas V Hud and Loren Dean Williams

Address
School of Chemistry and Biochemistry, Parker H. Petit Institute for Bioengineering and Bioscience, Center for Ribosomal Origins and Evolution, Georgia Institute of Technology, Atlanta, GA 30332-0400, United States

Corresponding author: Williams, Loren Dean (loren.williams@chemistry.gatech.edu)

Current Opinion in Structural Biology 2012, **22**:262–272

This review comes from a themed issue on
Nucleic acids
Edited by Jamie Williamson and Jody Puglisi

Available online 15th May 2012

0959-440X/$ – see front matter

http://dx.doi.org/10.1016/j.sbi.2012.04.006

Background

When large RNAs fold into compact structures, negatively charged phosphate groups are brought into close proximity. Compaction of RNA requires inorganic cations and polyamines that accumulate in and around the RNA envelope. The interactions of these cations with RNA are extremely subtle and polymorphic, and depend on the sequence and structure of the RNA, on the type of cation, and on other cations in the system. Mg^{2+} was seen early on to be especially important in tRNA folding [1–3]. It is now known that Mg^{2+} plays a reserved role in folding of essentially all large RNAs [4–6]. Some ribozymes appear to utilize Mg^{2+} ions to assist directly for stabilizing transition states [7,8].

Why Mg^{2+}?

Mg^{2+} is uniquely suited as a partner for RNA. Magnesium is the dominant divalent cation in biological systems, and is widely available in the biosphere (2% of the earth's crust). Mg^{2+} is highly soluble near neutral pH [K_{sp} of $Mg(OH)_2 = 10^{-12}$] and is inert to O_2.

Coordination of Mg^{2+} by water

Mg^{2+} orients and polarizes first shell water molecules, activating them for molecular recognition and enzymatic mechanism. Mg^{2+} is small with high charge density [$Mg^{2+}_{r_o}$ (ionic radius) = 0.65 Å, $Ca^{2+}_r = 0.99$Å, $Na^{+}_r = 0.95$Å, $K^{+}_r = 1.52$Å] [9–12]. In water, the first coordination shell of Mg^{2+} contains six tightly packed water molecules with highly constrained octahedral geometry. These water molecules are acidic, with elevated hydrogen-bond donating potential [pK_a of $Mg^{2+}(H_2O)_6 = 11.4$, pK_a of $Na^{+}(H_2O)_{6-8} = 14.4$, p$K_a$ of $H_2O_{bulk} = 15.7$] [13]. They are also compressed and electro-restricted, giving a large negative partial molal volume to Mg^{2+} in water ($Mg^{2+}_V = -30$ ml/mol; $Na^{+}_V = -5.7$ ml/mol) [14]. The oxygen atoms of the waters are directed inwards toward the metal center and the acidic protons are directed outwards. The dynamics of these water molecules are suppressed. The exchange of water from the first shell of Mg^{2+} is nearly four orders of magnitude slower, for example, than from the first shell of Na^{+} [15]. The enthalpy of hydration of Mg^{2+} is very large in magnitude (−450 kcal/mol) compared to other relevant cations (Na^{+}, −100 kcal/mol) [10].

Coordination of Mg^{2+} by RNA

Mg^{2+} can increase local rigidity of RNA by tightly packing functional groups in its first coordination shell (Figure 1). Phosphate groups, the preferred RNA ligands to Mg^{2+}, are significantly more polarizable than water molecules. When a phosphate oxygen of RNA enters the first shell of a Mg^{2+}, the attached phosphorus atom is activated to nucleophilic attack because electron density is pulled into the Mg^{2+}. Therefore, Mg^{2+} increases rates of RNA hydrolysis. In some cases the literature reveals a failure to distinguish dehydration from exchange. The enthalpy of exchange of a first shell water molecule for a phosphate oxygen is close to zero, even though the dehydration enthalpy is highly unfavorable.

The ratio of Mg^{2+} hydrate volume [V_h = the volume of $Mg^{2+}(H_2O)_6$] to ionic volume (V_i = the volume of Mg^{2+} alone) is especially large ($V_h/V_i = 400$) compared to that of Na^{+} ($V_h'/V_i' = 25$) and other relevant cations [11]. Therefore, the effects of Mg^{2+} dehydration on RNA structure are particularly acute. Mg^{2+} prefers oxygen ligands, although nitrogen ligands are observed in some systems (e.g. hemes). By way of similar size and charge density Mn^{2+} can reasonably substitute for Mg^{2+} in many experimental systems, although the lower-energy d-orbitals of Mn^{2+} have significant effects. Mn^{2+} is a trace element in biology and has little relevance to RNA folding *in vivo*.

Diffuse and site-bound cations

Common practice is to conceptually partition cations in the RNA envelope into two limiting modes, called diffuse and site-bound [16]. Diffuse cations are abundant and interact with RNA via weak but numerous long-range electrostatic interactions while remaining hydrated, and retaining near bulk-solution like mobility. Diffuse cations, by their overwhelmingly larger populations,

Figure 1

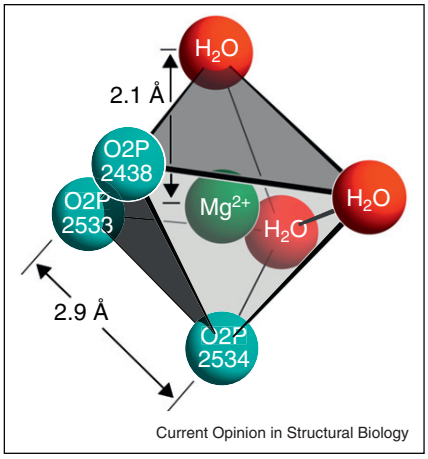

A Mg^{2+} ion chelated by RNA (Mg^{2+} 8001 from 23S rRNA of the *Haloarcula* LSU; PDB entry 1JJ2). This Mg^{2+} ion (green sphere) is octahedral, with three first shell phosphate oxygens of the rRNA (cyan) and three first shell water oxygens (red). Mg^{2+}-oxygen distances are around 2.1 Å. Mg^{2+} coordination tightly packs oxygen atoms, imposing oxygen–oxygen distances of around 2.9–3.2 Å. For clarity the radii of the spheres are reduced from the van der Waals radii of the atoms, and have no physical significance. Adapted from [51].

make the primary contributions to stability of compact RNAs. Site-bound ions interact strongly with the RNA at short distances, which vary depending on the type of cation. The mobilities of site-bound ions are low, and are often determined by those of the RNA itself. Highly chelated ions, with two or more first shell ligands contributed by RNA, are the least abundant but in some cases make important contributions to specific local or even global conformations. Site-bound ions are often required to access the native state. Site-bound cations are sometimes elevated to artificial significance by way of being readily observable by physical techniques. Many aspects of RNA electrostatics have been reviewed recently [6–8,17–25,26••].

Thinking beyond electrostatics

It has been stated that cations participate in RNA folding simply by balancing the self-repulsive negative charge of the RNA backbone during compaction. For weakly interacting cations like Na^+, K^+, polyamines, or hexahydrated Mg^{2+}, this simple electrostatic model can provide suitably accurate approximations of reality. This approximation fails for site-bound Mg^{2+} ions, which are distinct from complexes with other biologically available cations.

For Mg^{2+}, specific coordination chemistry and physics are important determinants of structure and stability. Site-bound Mg^{2+} ions compact, electro-restrict and polarize their first shell ligands, which interact with Mg^{2+} not only by electrostatic interactions but also by 'non-electrostatic' interactions including charge transfer, polarization and exchange correlation.

The local properties of RNA influence the interactions of Mg^{2+}. RNA chain flexibility, local positioning of phosphate groups, and charge density are important influences on site-binding of Mg^{2+} to RNA. Mg^{2+} forms site-bound complexes more readily with single-stranded RNA [27••,28] and compacted RNA than with double-stranded RNA.

How frequent are site-bound Mg^{2+} ions in folded RNAs? The ribosome provides a useful case study. Around 20% of RNA phosphate oxygens within 20 Å of the Peptidyl Transferase Center of the ribosomal Large Subunit (LSU) form first shell interactions with Mg^{2+} [29,30••]. By contrast, the RNA near the surface of the LSU shows very few first shell interactions with Mg^{2+}. So the frequency of site-bound Mg^{2+} in compact RNAs can be variable and idiosyncratic. RNA in the vicinity of catalytic sites tends to be Mg^{2+}-rich.

Energy decomposition reveals that first shell RNA-Mg^{2+} interactions have significant 'non-electrostatic' components, which are important determinants of structure and stability [31••]. Non-electrostatic components of the energy include polarization, charge transfer and exchange correlation (defined by Natural Energy Decomposition Analysis [32,33]). These components can be significant, and are determined by (i) the type of cation, (ii) the type of ligands contributed by the RNA, and (iii) the geometry of the coordination complex [31••,34,35••,36]. The net binding energy of a site-bound Mg^{2+} is composed of favorable electrostatic and 'non-electrostatic' components between cation and ligands balanced by unfavorable desolvation and ligand–ligand contributions (Figure 2).

The non-electrostatic components of site-bound interaction energies are larger and more important for Mg^{2+} [31••] than for other relevant cations. Non-electrostatic components are negligible for Na^+, K^+, Ca^{2+} and polyamines, because cation-ligand distances are long and cation charge densities lower.

It should be stressed that accurate atomistic predictions of geometries and energetics of compact RNAs in association with site-bound Mg^{2+} ions are essentially impossible by approaches that ignore non-electrostatic interactions [31••,34,35••,37,38], ion correlations [39,40], and the induction of specific RNA conformations by Mg^{2+} [31••,41]. Nonlinear Poisson–Boltzmann theory, Generalized Born approaches, and conventional Molecular Dynamics force fields have been used in most attempts to obtain all-atom or thermodynamic understanding of RNA folding in the presence of Mg^{2+}. The disconnect between these approximate theories and experimental

Figure 2

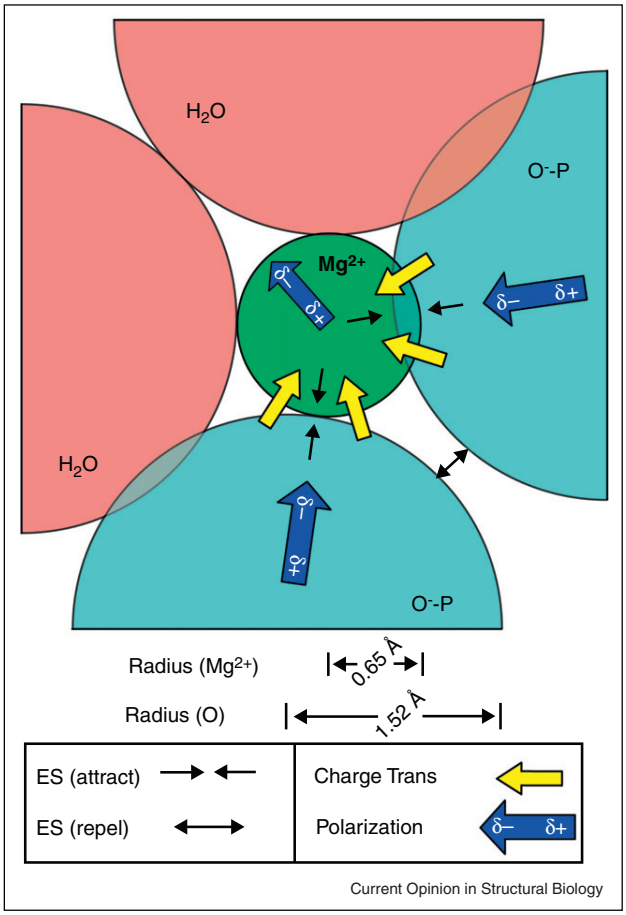

Interactions of a magnesium ion with two anionic phosphate oxygen atoms of RNA and four water molecules (the axial water molecules are omitted for clarity). The arrows represent electrostatic, polarization, and charge transfer components of the interaction energy. Only the major components of the interaction energy are shown. The exchange term, which is favorable but significantly weaker than the charge transfer and polarization terms, is omitted from the schematic diagram for clarity. The atoms are colored as in Figure 1. The interaction arrows are not to scale. Adapted from [31].

results is recognized [31••,34,35••,37,38] and has been experimentally demonstrated [42••]. These theoretical methods treat molecular interactions in very approximate ways. Site-bound Mg^{2+} ions require more rigorous methods, for example, a combined quantum mechanical/molecular mechanical (QM/MM) approach [36,43]. This approach is gaining broad use for characterization of ribozyme reaction coordinates [44–48], but not as of yet for RNA folding reaction pathways. Other polarizable models for RNA are on the horizon, and are being developed for small systems such as small ion-water clusters [49]. The rugged landscapes of RNA folding, with heterogeneous and parallel pathways [18], will continue to present extreme challenges to computational and theoretical approaches.

Mg^{2+}-specific conformation of RNA

Large RNAs can assume compact and near-native structures in the presence of monovalent cations, in the absence of Mg^{2+}. These quasi-folded RNAs contain native-like RNA-RNA tertiary interactions (i.e. native long-range base–base interactions) but are not true native states. They lack sites for chelated Mg^{2+} ions [50], which assemble only in the presence of Mg^{2+}. RNA conformation and site-specific Mg^{2+} binding are interdependent. In the absence of Mg^{2+}, RNA cannot enter certain conformation spaces – including those required for multidentate chelation of Mg^{2+}. In other words, Mg^{2+} stabilizes certain RNA conformations that are very unfavorable in the presence of monovalent cations alone, even at very high concentrations.

The Mg^{2+} clamp [31••,41] can be used to illustrate how RNA assembles around Mg^{2+} to build a binding site. A Mg^{2+} clamp is formed by two phosphates from adjacent nucleotides. Both penetrate the first shell of a common Mg^{2+} ion (Figures 3 and 4). Williams and co-workers have identified the Mg^{2+} clamp as the most frequent mode of bidentate chelation of Mg^{2+} by large RNAs [31••,41,51]. Twenty-five Mg^{2+} clamps are found in the *Haloarcula marismortui* LSU [PDB entry 1JJ2, ref. [52]], two in the P4–P6 domain of the *Tetrahymena* Group I intron [PDB

Figure 3

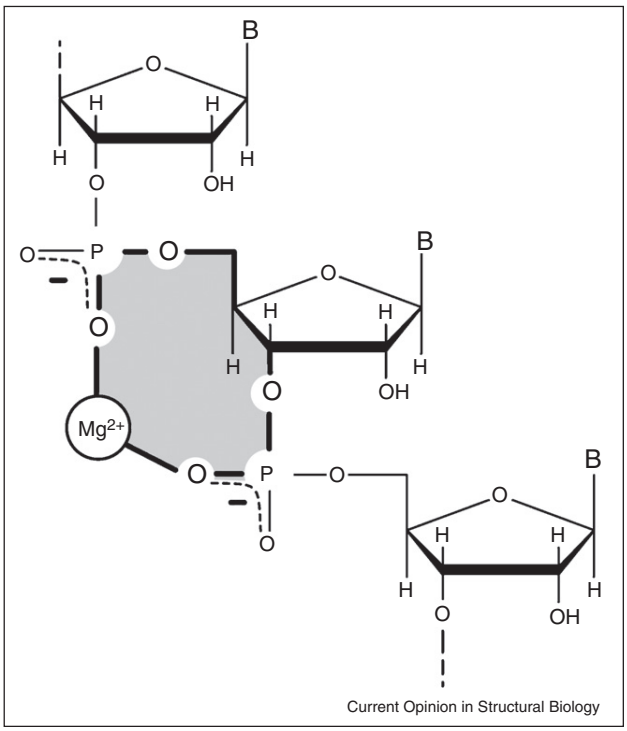

A schematic diagram of a bidentate RNA clamp of magnesium, formed when adjacent phosphate groups enter the first coordination shell of a common magnesium ion. A 10-membered ring (shaded) characterizes the Mg^{2+} clamp. Adapted from [31].

Figure 4

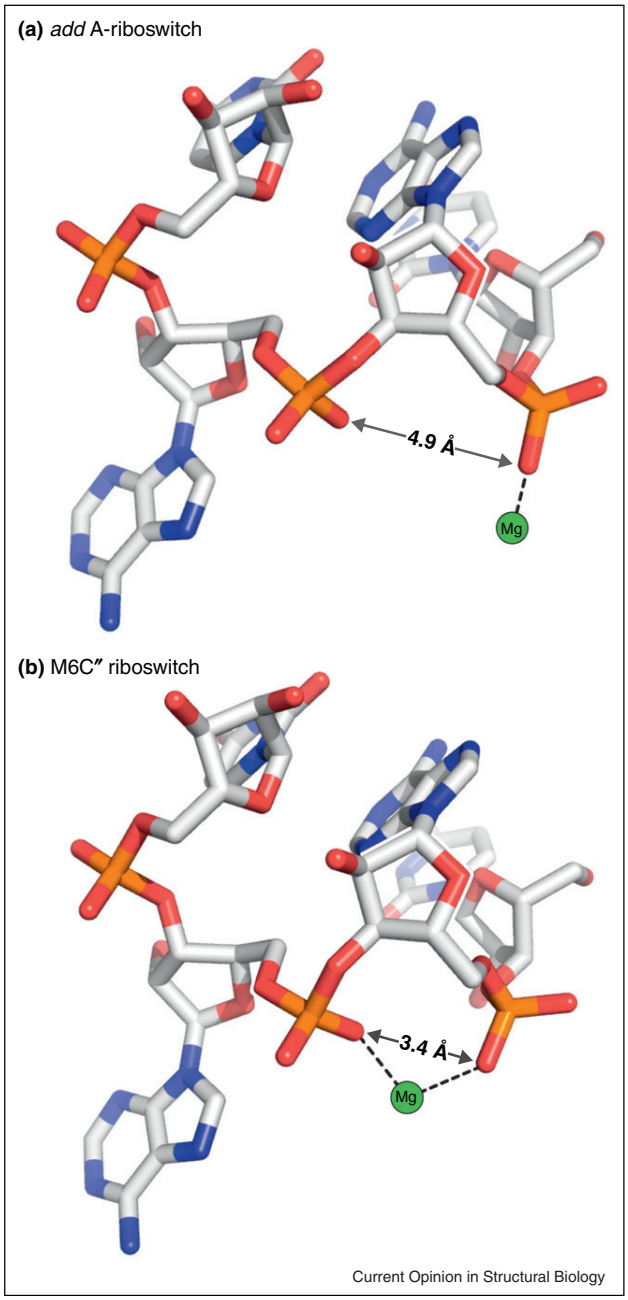

Assembly of a Mg^{2+} clamp. **(A)** The structure of the *add* A-riboswitch, which lacks a Mg^{2+} clamp (PDB entry 1Y26) is not in correct conformation for multidentate Mg^{2+} binding. **(B)** The structure of the synthetic riboswitch MC6″, which contains a Mg^{2+} clamp (PDB entry 3LA5). Mg^{2+} ions are green spheres.

entry 1GID, ref. [53,54]], one in a self-splicing Group II intron from *Oceanobacillus iheyensis* [PDB entry 3IGI, described in [55]], one in the *in vitro* evolved L1 ligase [PDB entry 2OIU, ref. [56]], and one in the synthetic M6C″ riboswitch [PDB entry 3LA5, ref. [57]].

One can infer the effects of Mg^{2+} on RNA conformation by comparing three-dimensional structures in which, effectively, a Mg^{2+} ion is added to a potential Mg^{2+}-clamp site on the RNA, inducing conformational change associated with formation of the clamp. The naturally occurring *add* A-riboswitch [58] and the synthetic riboswitch M6C″ [57] offer such a pair of structures. Draper has studied the Mg^{2+} interactions of the *add* A-riboswitch in solution and obtained an estimate of the folding energy landscape as a function of Mg^{2+} [59]. The synthetic M6C″ riboswitch differs from the *add* A-riboswitch by six nucleotide substitutions. The *add* A-riboswitch lacks a Mg^{2+} clamp involving A(23) and A(24) (Figure 4A) while M6C″ contains a clamp at that site (Figure 4B). One can infer, by comparing these structures, that upon formation of a Mg^{2+} clamp, phosphate oxygens are forced into close proximity, into direct van der Waals contact (3.4 Å). The repulsive interaction between these two anionic oxygen atoms is overcome by favorable interactions between these oxygen atoms and the Mg^{2+} ion (as shown in Figure 2). The ligands of the Mg^{2+} assume the geometry required for first shell Mg^{2+} coordination, a tightly packed octahedron (Figure 1) [9,60]. Tight packing and crowding are a hallmark of first shell magnesium ligands, leading to highly restrained geometry and strong ligand–ligand interactions. This conformation, with strong repulsion between the oxygen atoms, is not accessible to RNA in the absence of Mg^{2+}. Ion-specific RNA conformations, along with non-electrostatic effects of Mg^{2+} interactions, make thermodynamic and computational analysis of RNA electrostatics a challenging endeavor. Furthermore, thermodynamic interpretations of Mg^{2+} titrations have typically assumed constant RNA conformation [59]. However, since Mg^{2+} binding and Mg^{2+} binding site assembly are coupled (Figure 4), this assumption is unjustified for RNAs with highly coordinated Mg^{2+} ions. These subtle conformational changes are near the limit of detection of low resolution folding techniques such as SAXS [61].

Conceptual frameworks

The partitioning of cations into two modes (diffuse and site-bound) is useful for many applications, but is limiting in the sense that many cations fall between these two classes. We partition ions in association with RNA and DNA into four classes: free, condensed, glassy and chelated. The continuum nature of the phenomena and interdependence of parameters characterizing the four classes are illustrated schematically in Figure 5, while 3D structures are illustrated in Figure 6. The cation classes are circumscribed by relative populations, extent of coordination, rates and dimensionality of diffusion, thermodynamic contributions to stability, and influence on specific structural states (Figure 5). There are many more condensed ions than glassy or chelated ions (Figure 5A). For monovalent cations, the number of first shell ligands contributed by a nucleic acid can vary from zero (condensed) to six (chelated), eight in the case of the

Figure 5

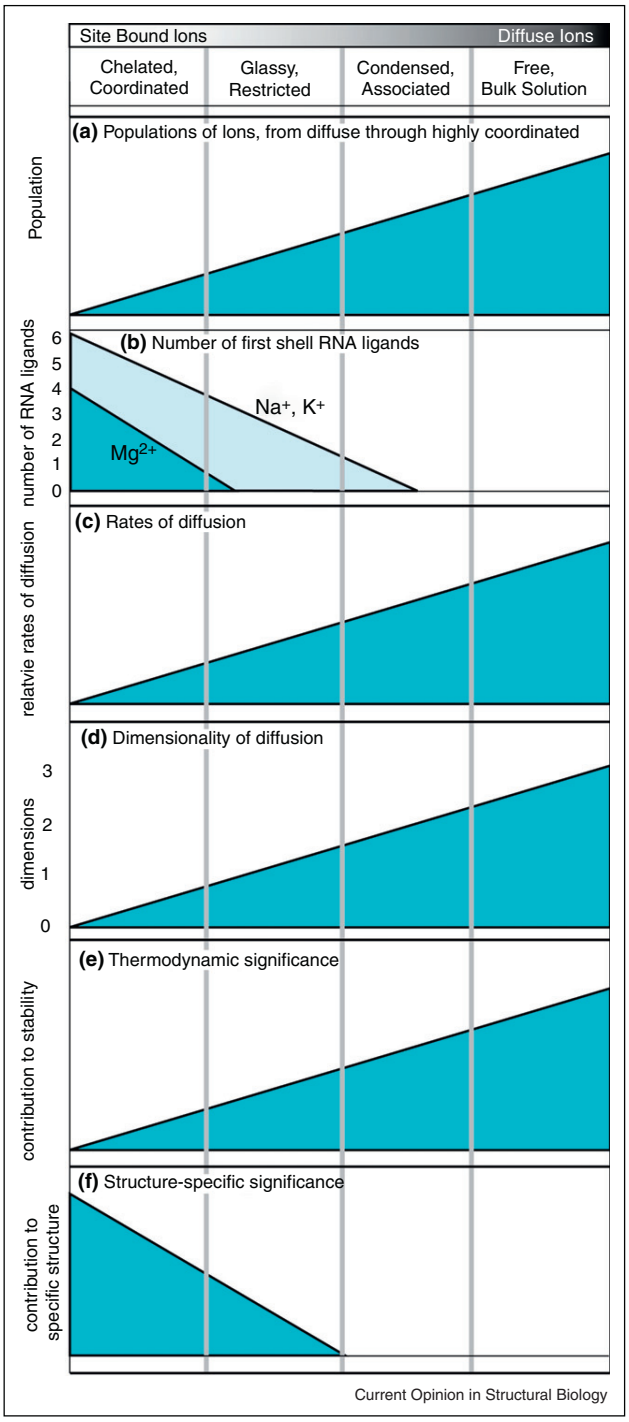

Schematic illustration of parameters describing RNA-cation interactions. **(A)** The population of diffuse cations is much greater than the population of site-bound cations. **(B)** Diffuse ions are not directly coordinated by RNA. The number of first shell ligands contributed by RNA to Na^+ or K^+ can generally vary from zero to six. In G-quadruplexes, monovalent cations are coordinated by up to eight first shell ligands from DNA or RNA. The number of first shell ligands contributed by RNA to Mg^{2+} can vary from zero to four. **(C)** As the number of first shell ligands contributed by RNA increases, the rate of diffusion of the cation decreases. **(D)** As the number of first shell ligands contributed by RNA increases, the dimensionality of diffusion of the cation decreases. For example, cations in the grooves of RNA are not free to diffuse in three dimensions. **(E)** As the number of first shell ligands contributed by RNA increases, the thermodynamic significance of cation association decreases, primarily because the number of cations with first shell RNA ligands is relatively small. **(F)** The specific structural significance of a cation increases with the number of first shell RNA ligands. We thank Drs. Gene Lamm and Anton Petrov for helpful discussions.

G-quadruplex motif, while for Mg^{2+}, the number of first shell ligands contributed by the RNA can vary from zero to four (Figure 5B). Envelopes containing condensed cations extend well beyond the van der Waals surface of the collapsed nucleic acid. These envelopes of condensed cations are illustrated in Figure 6B and G by isosurfaces for the densities of mobile charges, which were calculated using the Poisson–Boltzmann equation as implemented in APBS [62] for a solution of 100 mM KCl, 20 mM $MgCl_2$, with a 1.4 Å solvent probe at 298 °C.

Glassy ions are found closely associated with DNA or RNA (Figure 6C and H). The number of first shell nucleic acid ligands is higher for glassy monovalent cations than for glassy Mg^{2+} ions (Figures 5B, 6D and I). A Mg^{2+} ion with one first shell nucleic acid ligand (Figure 6D), or a monovalent cation with 4–5 first shell nucleic acid ligands, is in a glassy state (Figure 6I). Chelated Mg^{2+} ions, with three first shell RNA ligands, are shown in Figure 6E. The RNA conformation is specifically dependent on the positions and coordination of these Mg^{2+} ions. A chelated K+ ion with eight first shell DNA ligands, and no water ligands, is shown in Figure 6J. The DNA conformation is specifically dependent on the positions and coordination of this K^+ ion. The greater the number of first shell nucleic acid ligands, the slower the rate of diffusion (Figure 5C). Therefore, there are more cations in the condensed envelope with high rates of diffusion than with low rates of diffusion. The dimensionality of diffusion will track the rate of diffusion (Figure 5D) because cations in bulk solution diffuse freely in three dimensions while movement of cations within the grooves, for example, is more restrained; some cations within the grooves are glassy, with limited rates and dimensionality of diffusion. Increasing the number of first shell nucleic acid ligands decreases both the rate and dimensionality of diffusion. Chelated, fully dehydrated cations, such as monovalent cations contained within G-quadruplexes (Figure 6J), show very limited rates and dimensionality of diffusion. Thermodynamic significance to folding of the ground state structure is illustrated in Figure 5E. The number of cations with few or no first shell RNA ligands greatly exceeds the number with multiple first shell ligands, and therefore the net thermodynamic contribution to folding decreases with decreasing number of first shell RNA ligands. Small numbers of ions are highly chelated by the nucleic acid (Figures 5F, 6E and J), but

Figure 6

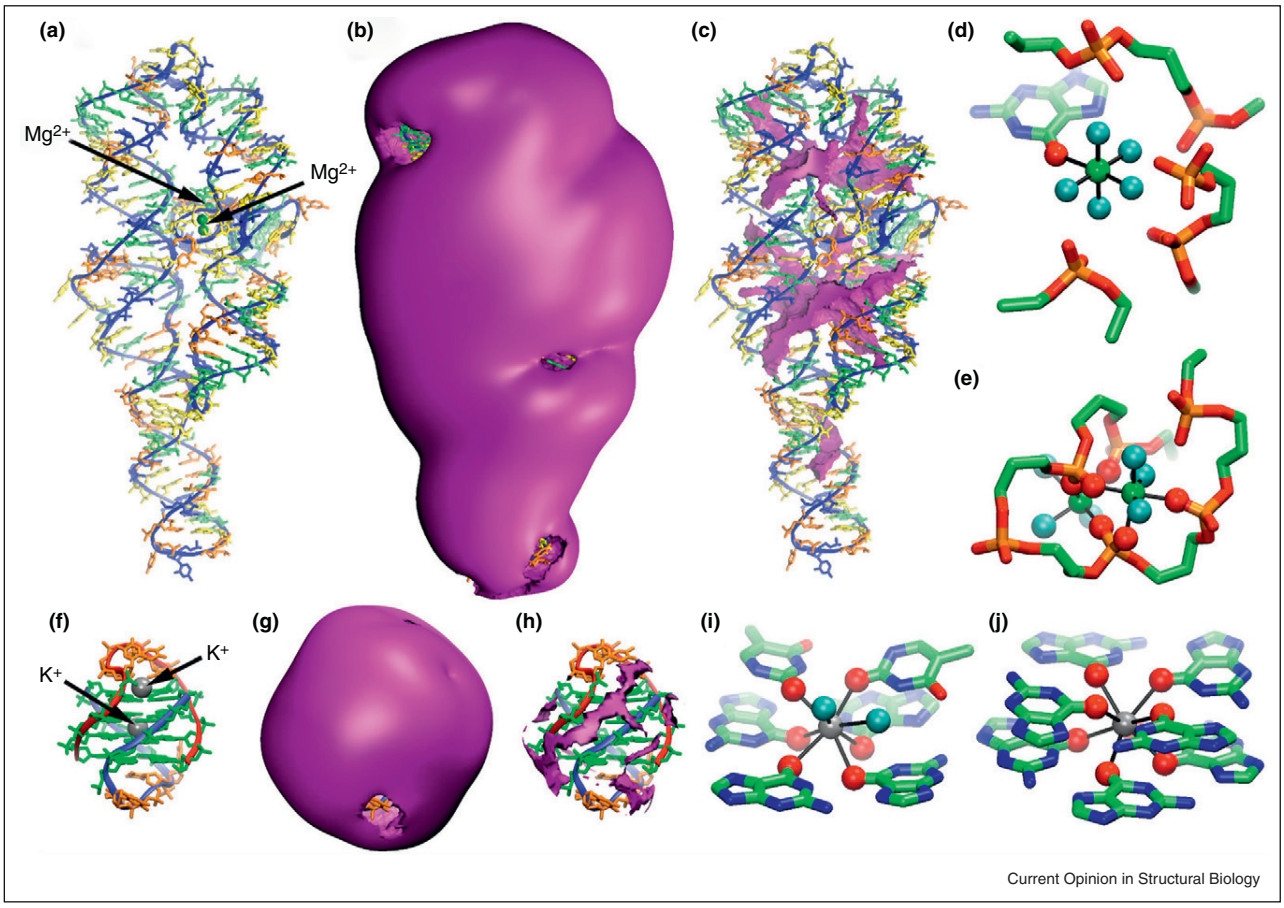

Condensed, glassy, and coordinated cations. **(A)** The structure of the P4–P6 domain of the *Tetrahymena* Group 1 intron RNA [PDB entry 1HR2]. Three Mg^{2+} ions are indicated by green spheres. The coordination of these ions is shown in detail in panels **D** and **E**. **(B)** The envelope containing condensed cations surrounding the P4–P6 RNA. This envelope was calculated with a mobile charge density of +0.5 M*e*. Ions within this envelope are well-hydrated, with near bulk-like diffusion properties. **(C)** Regions of glassy cation localization within the grooves, calculated with a mobile charge density of +5.0 M*e*. **(D)** Coordination of a glassy Mg^{2+} ion. This ion is coordinated by RNA and five water molecules. The rate and dimensionality of diffusion of this cation are restricted. A guanine base and selected backbone atoms of RNA are shown to illustrate positions and orientations of the second coordination shell of the Mg^{2+} ion (phosphorus, orange; oxygen, red; carbon, green; nitrogen, blue). Oxygen atoms of first-shell water molecules are cyan [Mg^{2+} 6766 of 1HR2]. **(E)** Highly coordinated Mg^{2+} ions induce specific conformational states of RNA. Two trichelate Mg^{2+} ions contain tightly packed RNA phosphate oxygen atoms in their first coordination shells [Mg^{2+} ions 6756 and 6758 of 1HR2]. **(F)** Structure of the G-quadruplex formed by $[d(G_4T_4G_4)]_2$ [PDB entry 1L1H]. K^+ ions are silver spheres. The coordination of these ions is shown in detail in panels **I** and **J**. **(G)** The envelope of condensed cations surrounding $[d(G_4T_4G_4)]_2$. The surface is calculated for a mobile charge density of +0.5 M*e*. **(H)** Predicted regions of glassy cation localization are illustrated by the iso-surface for a mobile charge density of +1.5 M*e*. **(I)** A glassy K^+ ion with first coordination shell ligands contributed by four guanine bases of a G-tetrad and two thymine bases [K^+ ion 6013 of 1L1H]. **(J)** A fully dehydrated, chelated K^+ ion coordinated by eight guanine oxygen atoms of two adjacent G-tetrads [K^+ 6015 of 1L1H]. In panels **D**, **E**, **I** and **J**, the radii of the atom spheres are reduced from their van der Waals/ionic radii for clarity.

these ions are most important to stabilizing specific three-dimensional structure, and cannot be substituted by other ion-types.

Quadruplexes: a well-defined case study in cation association

Differences among contributions of chelated, glassy, condensed and free ions to thermodynamics, kinetics and structure, as well as the difficulty in characterizing cations associated with a macromolecule in the solution state, are all illustrated by the extensive NMR spectroscopy investigations of cation binding to G-quadruplex DNA [63]. Within each G-quadruplex two or more stacked G-tetrads directly coordinate fully dehydrated monovalent cations (e.g. Na^+, K^+, NH_4^+) (Figure 6F and J). These chelated cations are coordinated by 6–8 first shell ligands contributed by the DNA. The development of $^{15}NH_4^+$ as an NMR probe of monovalent cation localization in solution allowed the direct characterization of these chelated cations in the quadruplex formed by $[d(G_4T_4G_4)]_2$.

These chelated cations, with residence times of around 250 ms, are in slow exchange on the NMR time scale with other cations [64]. Condensed cations on the outside of the G-quadruplex, with residences times of <1 ms, are in fast exchange with bulk solution cations, as indicated by resonance line broadening of the bulk $^{15}NH_4^+$ ^1H resonance [64]. Recent work by Ida and Wu using ^{23}Na NMR spectroscopy reveals glassy cations associated with the dT_4 loops of $[d(G_4T_4G_4)]_2$, with residence times that are intermediate between the chelated and condensed cations [65]. Surprisingly, the initial $^{15}NH_4^+$ probe did not provide evidence for these glassy cations, despite chemical shift evidence of cation-specific loop conformations [66]. In retrospect, all three modes of cation binding to the bimolecular G-quadruplex formed by $[d(G_4T_4G_4)]_2$ fit well with the conceptual framework presented in Figure 5. Specifically, G-quadruplex structure is most sensitive to the species of cation coordinated within the G-tetrads, being stable in the presence of monovalent cations with an ionic radius between that of Na^+ and Rb^+, but unstable when the only cation in solution with the DNA is either smaller (i.e. Li^+) or larger (i.e. Cs^+) than Na^+ or Rb^+ [63]. Furthermore, charge repulsions between the phosphate backbones of a G-quadruplex can, in general, be screened by Li^+ or Cs^+ in place of Na^+ or K^+ with little change in G-quadruplex structure, whereas substitution of Na^+ by K^+ or NH_4^+ causes detectable changes in the folded structure of $[d(G_4T_4G_4)]_2$ [66].

Ribozymes and Mg^{2+}

Initial expectations that ribozymes were obligate metalloenzymes [67] were undercut by observations of ribozyme activity in the absence of Mg^{2+} [68–70], the biological cation uniquely capable of assisting in catalysis. Full and accurate characterization of Mg^{2+} in catalytic systems remains a challenge, requiring a deconvolution of thermodynamic, structural and catalytic roles. Ward and DeRose [71••] recently focused on the hammerhead ribozyme, a heavily investigated RNA that spawned persistent disagreement about mechanism [72]. The hammerhead ribozyme cleaves RNA by nucleophilic attack of a 2′-OH on the proximal phosphorous atom. DeRose used a phosphorothioate/Cd^{2+} rescue system, in which sulfur was stereospecifically substituted for either non-bridging oxygen of the scissile phosphate. From differential cleavage rates of the two stereoisomers in the presence of Cd^{2+} it was concluded that the Pro-R_P oxygen of the scissile phosphate is a first shell ligand of Mg^{2+} in the ground-state of the ribozyme, in the native hammerhead *in vivo*. DeRose's model differs from a 'dynamic model,' in which a Mg^{2+} is recruited to the scissile phosphate at some point along the reaction coordinate. For the *glmS* ribozyme, Mg^{2+} appears to play a less direct role. Brooks and Hampel [73] studied Mg^{2+} contributions to mechanism by prefolding the *glmS* ribozyme into a native or near-native state. This folded RNA appears to bind substrate and Mg^{2+} without any conformational change, and directs catalysis very rapidly. The authors suggest that the sole obligatory role for Mg^{2+} is to assist in ligand binding, as suggested by a previous X-ray structure [74].

New methods

New applications of established techniques, combined with new technologies and computational capabilities, provide increasingly detailed views of RNA electrostatics and ion interactions.

Footprinting

The footprinting method SHAPE, developed and championed by Weeks [75], enjoys increasingly broad application for probing RNA secondary structure at nucleotide resolution. The Mg^{2+}-dependence of SHAPE reactivities appears to be quite general and informative, and has been demonstrated for tRNA [76], RNase P [77], and Domain III of the ribosomal LSU [78]. Several groups [79,80] are pursuing time-resolved chemical footprinting at nucleotide resolution by hydroxyl radical cleavage on increasingly large and complex RNA assemblies. This approach can detect time-dependent tertiary structure and protein interactions during folding and assembly. Local measures of folding can be combined with more global measures (SAXS, etc., see below) to give a comprehensive picture of folding pathways. We believe it will soon be possible to decompose Mg^{2+}-dependent RNA chemical reactivities into detailed descriptions of Mg^{2+} chelation by RNA.

SAXS, ASAXS, smFRET

Small angle X-ray scattering (SAXS) and anomalous SAXS (ASAXS) can be used to characterize conformations and ion distributions of nucleic acids at resolutions of ~10 Å [23]. SAXS provides information about the size, shape, compactness, and molecular weight of RNAs. ASAXS reports on diffuse cations, and has been used by Pollack and co-workers to differentiate monovalent cation distributions in B-form DNA and A-form RNA [81]. Single molecule Förster resonance energy transfer (smFRET) measures distances within or between RNAs (or DNAs). The Pollack group has studied the Mg^{2+}-dependence of properties of unstructured ssDNA and ssRNA with SAXS and smFRET [82••], and has detected that ssDNA and ssRNA have different conformations in solution, as expected from sugar pucker and stacking preferences. Of more relevance here, they find that for both ssRNA and ssDNA, charge screening by Mg^{2+} is anomalously efficient. Combined applications of SAXS/ASAXS/smFRET to more complex RNAs appear to be on the horizon.

Woodson and co-workers [61] monitored folding of the *Azoarcus* and *Tetrahymena* Group I ribozymes under various solution conditions by SAXS. Decreases in the radius of gyration (R_g) are observed upon addition of cations,

corresponding to collapse. The results suggest that total charge of the cations, not valence or charge density, is the most important characteristic for initial collapse. Polyamines induce the collapse of the *Azoarcus* ribozyme at mid-micromolar concentrations, Mg^{2+} induces collapse at high-micromolar concentrations, while monovalent cations induce collapse in the mid-millimolar range. Subtle differences in R_g for various ions demonstrate that even for a low resolution assay like SAXS, specific effects of Mg^{2+} on the collapsed state are observable. The collapsed state is slightly more compact with Mg^{2+} than with monovalents or polyamines. Although the ability of SAXS to reliably detect Mg^{2+}-specific effects on RNA folding remains an open question, these results support the model of collapse described above [50], in which RNA can collapse to a near native-state in the presence of Na^+, K^+ or polyamines. These compact RNAs can contain many native RNA-RNA tertiary interactions (i.e. native long-range base–base interactions) but may not be conformationally identical to RNA with site-bound Mg^{2+} ions.

Nesbitt and co-workers have used temperature-controlled smFRET to explore the Mg^{2+}-dependent thermodynamics and kinetics of RNA folding/unfolding in a model system [83••]. They observe that increasing [Mg^{2+}] promotes tetraloop–receptor interaction by reducing both the entropic activation barrier and the net entropy of the transition with minimal effects on activation enthalpy and net enthalpy. Their results appear to be consistent with a previous proposal [51] that during RNA folding, Mg^{2+} can form chelation complexes preferentially with flexible regions of RNA, locking out conformational heterogeneity.

Raman, EXAFS and NMR spectroscopies

New methods for characterizing site-bound cations in solution are emerging. Fierke and co-workers [84] report that a combination of extended X-ray absorption fine structure (EXAFS) and paramagnetic line-broadening experiments by NMR reveal a hexacoordinated Zn^{2+} interacting with a mimic of the conserved P4 helix of RNase P, with inner-sphere coordination at two specific residues (average Zn–O/N distance of 2.08 Å). Harris and co-workers [85] report attenuation of the Raman signal of symmetric vibrations of RNA non-bridging phosphate oxygens by electrostatic, hydrogen bond and inner-sphere interactions with metals. They also report cation-specific shifts (based on hardness and electronegativity) to higher wavenumbers with inner-sphere metal coordination.

Quasielastic neutron scattering spectroscopy

Woodson and co-workers used quasielastic neutron scattering spectroscopy to reach the counter-intuitive conclusion that Mg^{2+} *increases* tRNA dynamics on the picosecond to nanosecond timescale while stabilizing the folded state [86••]. For tRNA in a minimally hydrated state it seems that compaction can accompany increases in local molecular dynamics. The results suggest that water lubricates conformational motions of the macromolecules, but differences in the temperature dependencies of the mobilities of folded and unfolded tRNA were interpreted to suggest that dynamics are not controlled solely by hydrating water but are significantly affected by the electrostatic nature of the RNA surface. Specifically, charge screening by counterions increases the local motion of both tRNA and a synthetic charged polyelectrolyte that does not fold into a specific structure.

Computational and theoretical advances – the long and winding road

Using a simple experimental system designed to obtain interpretable data with the potential to validate or falsify various theories, Herschlag and co-workers measured the unfolding of a DNA hairpin [42••]. Measurements were made on single molecules with constrained conformations. The results show, as expected [31••,34,35••,37,38], that Poisson–Boltzmann theory can successfully account for Na^+-dependence but not Mg^{2+}-dependence of the stability of a simple folded DNA (other monovalent cations were also investigated). However, in the presence of Mg^{2+}, Poisson–Boltzmann Theory, which describes ions as non-interacting point charges, fails to correctly predict the energetics of DNA hairpin formation.

Herschlag speculates [42••] that ion–ion correlations [39,40] are an important contributor to the failure of Poisson–Boltzmann Theory to accurately predict stability in the presence of Mg^{2+}. To treat correlations, Chen [87••,88] has partitioned cations into bound and diffuse classes, and assigned the space occupied by the two classes of ions as bound regions and diffuse regions. This 'Tightly Bound Ion' (TBI) model successfully predicts that Mg^{2+} is more efficient than Na^+ at charge screening beyond considerations of ionic strength alone (also see [82••]). The high efficiency of Mg^{2+} screening is most pronounced for compact folded structures. The TBI method gives good agreement with experimentally observed salt dependence of stabilities for several model systems. However as noted by Chen, the model in its current form uses a minimal approximation of charge distribution of RNA and is limited to simple non-globular RNA structures. Additional developments of the TBI model are intended to include cation site-binding and associated dehydration effects. Applications of the model to large and complex RNA structures would involve sampling of very large ensembles of ion distributions, requiring a new computationally efficient sampling method.

Concluding remarks

The extent of recent literature underscores the importance and complexity of cation associations with RNA. We focused here on Mg^{2+} because it clearly plays a reserved,

ubiquitous and misunderstood role in RNA folding. Mg^{2+} is unique in that specific coordination chemistry and significant 'non-electrostatic' components of interaction energies are important determinants of structure and stability. Large RNAs can assume compact and near-native structures in the presence of monovalent cations alone, but these are not generally true native conformations. As illustrated here by the *add* A-riboswitch, RNA conformation is directly altered by multidentate chelation of Mg^{2+}. We propose that the two-state formalism of cation interactions (site-bound and diffuse) in many cases could be replaced to significant advantage by a genuinely continuous formalism or by a finer grained (chelated, glassy, condensed and free) formalism.

Acknowledgements

The Center for Ribosomal Origins and Evolution is supported by the NASA Astrobiology Institute.

References and recommended reading

Papers of particular interest, published within the period of review, have been highlighted as:

- • of special interest
- •• of outstanding interest

1. Stein A, Crothers DM: **Conformational changes of transfer RNA. The role of magnesium(II) equilibrium binding of magnesium(II) by Escherichia coli $tRNA^{fMet}$**. *Biochemistry* 1976, **15**:160-168.
2. Lynch DC, Schimmel PR: **Cooperative binding of magnesium to transfer ribonucleic acid studied by a fluorescent probe**. *Biochemistry* 1974, **13**:1841-1852.
3. Lindahl T, Adams A, Fresco JR: **Renaturation of transfer ribonucleic acids through site binding of magnesium**. *Proc Natl Acad Sci USA* 1966, **55**:941-948.
4. Brion P, Westhof E: **Hierarchy and dynamics of RNA folding**. *Annu Rev Biophys Biomol Struct* 1997, **26**:113-137.
5. Draper DE: **RNA folding: thermodynamic and molecular descriptions of the roles of ions**. *Biophys J* 2008, **95**:5489-5495.
6. Auffinger P, Grover N, Westhof E: **Metal ion binding to RNA**. *Met Ions Life Sci* 2011, **9**:1-35.
7. Butcher SE: **The spliceosome and its metal ions**. *Met Ions Life Sci* 2011, **9**:235-251.
8. Johnson-Buck AE, McDowell SE, Walter NG: **Metal ions: supporting actors in the playbook of small ribozymes**. *Met Ions Life Sci* 2011, **9**:175-196.
9. Brown ID: **Chemical and steric constraints in inorganic solids**. *Acta Crystallogr Sect B* 1992, **48**:553-572.
10. Rashin AA, Honig B: **Reevaluation of the born model of ion hydration**. *J Phys Chem* 1985, **89**:5588-5593.
11. Maguire ME, Cowan JA: **Magnesium chemistry and biochemistry**. *BioMetals* 2002, **15**:203-210.
12. Bock CW, Markham GD, Katz AK, Glusker JP: **The arrangement of first- and second-shell water molecules around metal ions: effects of charge and size**. *Theor Chem Acc* 2006, **115**:100-112.
13. Baes CF, Mesmer RE: *Hydrolysis of Cations*. New York: Wiley; 1976.
14. Serdyuk IN, Zaccai NR, Zaccai J: *Methods in Molecular Biophysics: Structure, Dynamics, Function*. Cambridge, UK: Cambridge University Press; 2007.
15. Diebler H, Eigen M, Ilgenfritz G, Maass G, Winkler R: **Kinetics and mechanism of reactions of main group metal ions with biological carriers**. *Pure Appl Chem* 1969, **20**:93-116.
16. Porschke D: **The mode of Mg^{++} binding to oligonucleotides. Inner sphere complexes as markers for recognition?** *Nucleic Acids Res* 1979, **6**:883-898.
17. Schurr JM: **Polyanion Models of Nucleic Acid–Metal Ion Interactions**. In *Nucleic Acid Metal Ion Interactions.* Edited by Hud N. The Royal Society of Chemistry; 2009:307-349.
18. Woodson SA: **Compact intermediates in RNA folding**. *Annu Rev Biophys* 2010, **39**:61-77.
19. Ramesh A, Winkler WC: **Magnesium-sensing riboswitches in bacteria**. *RNA Biol* 2010, **7**:77-83.
20. Erat MC, Sigel RK: **Methods to detect and characterize metal ion binding sites in RNA**. *Met Ions Life Sci* 2011, **9**:37-100.
21. Ferre-D'Amare AR, Winkler WC: **The roles of metal ions in regulation by riboswitches**. *Met Ions Life Sci* 2011, **9**:141-173.
22. Lassila JK, Zalatan JG, Herschlag D: **Biological phosphoryl-transfer reactions: understanding mechanism and catalysis**. *Annu Rev Biochem* 2011, **80**:669-702.
23. Pollack L: **SAXS studies of ion-nucleic acid interactions**. *Annu Rev Biophys* 2011, **40**:225-242.
24. Tan ZJ, Chen SJ: **Importance of diffuse metal ion binding to RNA**. *Met Ions Life Sci* 2011, **9**:101-124.
25. Wedekind JE: **Metal ion binding and function in natural and artificial small RNA enzymes from a structural perspective**. *Met Ions Life Sci* 2011, **9**:299-345.
26. •• Holm NG: **The significance of Mg in prebiotic geochemistry**. *Geobiology* 2012. [Epub ahead of print].
This is a unique and particularly interesting review of Mg^{2+} in the context of geobiology.
27. •• Kankia BI: **Binding of Mg^{2+} to single-stranded polynucleotides: hydration and optical studies**. *Biophys Chem* 2003, **104**:643-654.
Acoustic and density measurements were used to calculate the volume and compressibility effects of Mg^{2+} binding to single-stranded RNAs. The results are interpreted to indicate site binding of Mg^{2+} to single-stranded RNAs. Greater backbone flexibility is associated with greater site binding of Mg^{2+}.
28. Kankia BI: **Inner-sphere complexes of divalent cations with single-stranded poly(rA) and poly(rU)**. *Biopolymers* 2004, **74**:232-239.
29. Hsiao C, Mohan S, Kalahar BK, Williams LD: **Peeling the onion: ribosomes are ancient molecular fossils**. *Mol Biol Evol* 2009, **26**:2415-2425.
30. •• Klein DJ, Moore PB, Steitz TA: **The contribution of metal ions to the structural stability of the large ribosomal subunit**. *RNA* 2004, **10**:1366-1379.
This paper, and ribosome structures in general, demonstrate the importance of highly coordinated Mg^{2+} ions in large RNA structures.
31. •• Petrov AS, Bowman JC, Harvey SC, Williams LD: **Bidentate RNA-magnesium clamps: on the origin of the special role of magnesium in RNA folding**. *RNA* 2011, **17**:291-297.
This work shows that a frequent motif for site-bound magnesium–RNA complexes cannot be accurately described by simple electrostatic models. Polarization and charge transfer are important components of energetics of site-bound Mg^{2+} ions.
32. Glendening ED: **Natural energy decomposition analysis: explicit evaluation of electrostatic and polarization effects with application to aqueous clusters of alkali metal cations and neutrals**. *J Am Chem Soc* 1996, **118**:2473-2482.
33. Schenter GK, Glendening ED: **Natural energy decomposition analysis: the linear response electrical self energy**. *J Phys Chem* 1996, **100**:17152-17156.
34. Rulisek L, Sponer J: **Outer-shell and inner-shell coordination of phosphate group to hydrated metal ions (Mg^{2+}, Cu^{2+}, Zn^{2+}, Cd^{2+}) in the presence and absence of nucleobase. The role of nonelectrostatic effects**. *J Phys Chem B* 2003, **107**:1913-1923.
35. •• Petrov AS, Pack GR, Lamm G: **Calculations of magnesium-nucleic acid site binding in solution**. *J Phys Chem B* 2004, **108**:6072-6081.

The authors demostrate that a major drawback of MD, NLPB and other applications of simplified force fields for characterizing Mg^{2+} interactions with RNA is a failure to account for non-electrostatic components of the interaction energies. The most important neglected terms are charge transfer and polarization.

36. Ditzler MA, Otyepka M, Sponer J, Walter NG: **Molecular dynamics and quantum mechanics of RNA: conformational and chemical change we can believe in**. *Acc Chem Res* 2010, **43**:40-47.

37. Gresh N, Sponer JE, Spackova N, Leszczynski J, Sponer J: **Theoretical study of binding of hydrated Zn(II) and Mg(II) cations to 5′-guanosine monophosphate. Toward polarizable molecular mechanics for DNA and RNA**. *J Phys Chem B* 2003, **107**:8669-8681.

38. Petrov AS, Lamm G, Pack GR: **Calculation of the binding free energy for magnesium-RNA interactions**. *Biopolymers* 2005, **77**:137-154.

39. Heilman-Miller SL, Thirumalai D, Woodson SA: **Role of counterion condensation in folding of the Tetrahymena ribozyme. I. Equilibrium stabilization by cations**. *J Mol Biol* 2001, **306**:1157-1166.

40. Chu VB, Herschlag D: **Unwinding RNA's secrets: advances in the biology, physics, and modeling of complex RNAs**. *Curr Opin Struct Biol* 2008, **18**:305-314.

41. Hsiao C, Williams LD: **A recurrent magnesium-binding motif provides a framework for the ribosomal peptidyl transferase center**. *Nucleic Acids Res* 2009, **37**:3134-3142.

42. •• Anthony PC, Sim AY, Chu VB, Doniach S, Block SM, Herschlag D: **Electrostatics of nucleic acid folding under conformational constraint**. *J Am Chem Soc* 2012, **134**:4607-4614.
The data presented here show that current theories fail to predict the effects of Mg^{2+} on folding and stability of simple RNAs. The data provide benchmarks for developing theories for quantitative and predictive understanding of folding.

43. Banas P, Jurecka P, Walter NG, Sponer J, Otyepka M: **Theoretical studies of RNA catalysis: hybrid QM/MM methods and their comparison with MD and QM**. *Methods* 2009, **49**:202-216.

44. Rosta E, Nowotny M, Yang W, Hummer G: **Catalytic mechanism of RNA backbone cleavage by ribonuclease H from quantum mechanics/molecular mechanics simulations**. *J Am Chem Soc* 2011, **133**:8934-8941.

45. Veeraraghavan N, Ganguly A, Chen JH, Bevilacqua PC, Hammes-Schiffer S, Golden BL: **Metal binding motif in the active site of the HDV ribozyme binds divalent and monovalent ions**. *Biochemistry* 2011, **50**:2672-2682.

46. Mlýnský V, Banáš P, Walter NG, Šponer J, Otyepka M: **QM/MM studies of hairpin ribozyme self-cleavage suggest the feasibility of multiple competing reaction mechanisms**. *J Phys Chem B* 2011, **115**:13911-13924.

47. Lee TS, Giambasu G, Harris ME, York DM: **Characterization of the structure and dynamics of the HDV ribozyme at different stages along the reaction path**. *J Phys Chem Lett* 2011, **2**:2538-2543.

48. Sgrignani J, Magistrato A: **The structural role of mg^{2+} ions in a class I RNA polymerase ribozyme: a molecular simulation study**. *J Phys Chem B* 2012, **116**:2259-2268.

49. Yu H, Whitfield TW, Harder E, Lamoureux G, Vorobyov I, Anisimov VM, Mackerell AD Jr, Roux B: **Simulating monovalent and divalent ions in aqueous solution using a Drude polarizable force field**. *J Chem Theory Comput* 2010, **6**:774-786.

50. Takamoto K, Das R, He Q, Doniach S, Brenowitz M, Herschlag D, Chance MR: **Principles of RNA compaction: insights from the equilibrium folding pathway of the P4–P6 RNA domain in monovalent cations**. *J Mol Biol* 2004, **343**:1195-1206.

51. Hsiao C, Tannenbaum M, VanDeusen H, Hershkovitz E, Perng G, Tannenbaum A, Williams LD: **Complexes of nucleic acids with group I and II cations**. In *Nucleic Acid Metal Ion Interactions.* Edited by Hud N. The Royal Society of Chemistry; 2009:1-35.

52. Ban N, Nissen P, Hansen J, Moore PB, Steitz TA: **The complete atomic structure of the large ribosomal subunit at 2.4 Å resolution**. *Science* 2000, **289**:905-920.

53. Cate JH, Hanna RL, Doudna JA: **A magnesium ion core at the heart of a ribozyme domain**. *Nat Struct Biol* 1997, **4**:553-558.

54. Juneau K, Podell E, Harrington DJ, Cech TR: **Structural basis of the enhanced stability of a mutant ribozyme domain and a detailed view of RNA–solvent interactions**. *Structure* 2001, **9**:221-231.

55. Toor N, Keating KS, Taylor SD, Pyle AM: **Crystal structure of a self-spliced group II intron**. *Science* 2008, **320**:77-82.

56. Robertson MP, Scott WG: **The structural basis of ribozyme-catalyzed RNA assembly**. *Science* 2007, **315**:1549-1553.

57. Dixon N, Duncan JN, Geerlings T, Dunstan MS, McCarthy JE, Leys D, Micklefield J: **Reengineering orthogonally selective riboswitches**. *Proc Natl Acad Sci USA* 2010, **107**:2830-2835.

58. Serganov A, Yuan YR, Pikovskaya O, Polonskaia A, Malinina L, Phan AT, Hobartner C, Micura R, Breaker RR, Patel DJ: **Structural basis for discriminative regulation of gene expression by adenine- and guanine-sensing mRNAs**. *Chem Biol* 2004, **11**:1729-1741.

59. Leipply D, Draper DE: **Effects of Mg^{2+} on the free energy landscape for folding a purine riboswitch RNA**. *Biochemistry* 2011, **50**:2790-2799.

60. Bock CW, Katz AK, Markham GD, Glusker JP: **Manganese as a replacement for magnesium and zinc: functional comparison of the divalent ions**. *J Am Chem Soc* 1999, **121**:7360-7372.

61. Moghaddam S, Caliskan G, Chauhan S, Hyeon C, Briber RM, Thirumalai D, Woodson SA: **Metal ion dependence of cooperative collapse transitions in RNA**. *J Mol Biol* 2009, **393**:753-764.

62. Dolinsky TJ, Nielsen JE, McCammon JA, Baker NA: **PDB2PQR: an automated pipeline for the setup of Poisson–Boltzmann electrostatics calculations**. *Nucleic Acids Res* 2004, **32**:W665-W667.

63. Engelhart AE, Plavec J, Persil O, Hud NV: **Metal ion interactions with G-quadruplex structures**. In *Nucleic Acid Metal Ion Interactions.* Edited by Hud N. The Royal Society of Chemistry; 2009:118-153.

64. Hud NV, Schultze P, Sklenar V, Feigon J: **Binding sites and dynamics of ammonium ions in a telomere repeat DNA quadruplex**. *J Mol Biol* 1999, **285**:233-243.

65. Ida R, Wu G: **Direct NMR detection of alkali metal ions bound to G-quadruplex DNA**. *J Am Chem Soc* 2008, **130**:3590-3602.

66. Schultze P, Hud NV, Smith FW, Feigon J: **The effect of sodium, potassium and ammonium ions on the conformation of the dimeric quadruplex formed by the Oxytricha nova telomere repeat oligonucleotide $d(G_4T_4G_4)$**. *Nucleic Acids Res* 1999, **27**:3018-3028.

67. Steitz TA, Steitz JA: **A general two-metal-ion mechanism for catalytic RNA**. *Proc Natl Acad Sci USA* 1993, **90**:6498-6502.

68. Hampel A, Cowan JA: **A unique mechanism for RNA catalysis: the role of metal cofactors in hairpin ribozyme cleavage**. *Chem Biol* 1997, **4**:513-517.

69. Nesbitt S, Hegg LA, Fedor MJ: **An unusual pH-independent and metal-ion-independent mechanism for hairpin ribozyme catalysis**. *Chem Biol* 1997, **4**:619-630.

70. Murray JB, Seyhan AA, Walter NG, Burke JM, Scott WG: **The hammerhead, hairpin and VS ribozymes are catalytically proficient in monovalent cations alone**. *Chem Biol* 1998, **5**:587-595.

71. •• Ward WL, Derose VJ: **Ground-state coordination of a catalytic metal to the scissile phosphate of a tertiary-stabilized Hammerhead ribozyme**. *RNA* 2012, **18**:16-23.
From Cd^{2+} rescue DeRose concludes that the Pro-R_P oxygen of the scissile phosphate forms first shell interactions with a Mg^{2+} in the ground-state of the native ribozyme. This model differs from a 'dynamic model,' in which the Mg^{2+} is recruited to the scissile phosphate at some point along the reaction coordinate.

72. Scott WG: **Ribozymes**. *Curr Opin Struct Biol* 2007, **17**:280-286.

73. Brooks KM, Hampel KJ: **Rapid steps in the glmS ribozyme catalytic pathway: cation and ligand requirements**. *Biochemistry* 2011, **50**:2424-2433.

74. Klein DJ, Ferré-D'Amaré AR: **Structural basis of glmS ribozyme activation by glucosamine-6-phosphate**. *Science* 2006, **313**:1752-1756.

75. Weeks KM, Mauger DM: **Exploring RNA structural codes with SHAPE chemistry**. *Acc Chem Res* 2011, **44**:1280-1291.

76. Wilkinson KA, Merino EJ, Weeks KM: **RNA SHAPE chemistry reveals nonhierarchical interactions dominate equilibrium structural transitions in tRNA(Asp) transcripts**. *J Am Chem Soc* 2005, **127**:4659-4667.

77. Mortimer SA, Weeks KM: **Time-resolved RNA SHAPE chemistry**. *J Am Chem Soc* 2008, **130**:16178-16180.

78. Athavale SS, Gossett JJ, Hsiao C, Bowman JC, Neill EB, Hershkovitz E, Preeprem T, Hud NV, Wartell RM, Harvey SC, Williams LD: **Domain III of the T. thermophilus 23S rRNA folds independently to a near-native state**. *RNA* 2012, **18**:752-758.

79. Woodson SA: **RNA folding pathways and the self-assembly of ribosomes**. *Acc Chem Res* 2011, **44**:1312-1319.

80. Schlatterer JC, Brenowitz M: **Complementing global measures of RNA folding with local reports of backbone solvent accessibility by time resolved hydroxyl radical footprinting**. *Methods* 2009, **49**:142-147.

81. Pabit SA, Qiu X, Lamb JS, Li L, Meisburger SP, Pollack L: **Both helix topology and counterion distribution contribute to the more effective charge screening in dsRNA compared with dsDNA**. *Nucleic Acids Res* 2009, **37**:3887-3896.

82. •• Chen H, Meisburger SP, Pabit SA, Sutton JL, Webb WW, Pollack L: **Ionic strength-dependent persistence lengths of single-stranded RNA and DNA**. *Proc Natl Acad Sci USA* 2012, **109**:799-804.
The application of unstructured polymer models for denatured state collapse are in agreement with static molecule SAXS scattering curves and dynamic molecule smFRET efficiencies.

83. •• Fiore JL, Holmstrom ED, Nesbitt DJ: **Entropic origin of Mg^{2+}-facilitated RNA folding**. *Proc Natl Acad Sci USA* 2012, **109**:2902-2907.
Mg^{2+} reduces both the entropy of activation and the net entropy of formation for a tetraloop–receptor complex.

84. Koutmou KS, Casiano-Negroni A, Getz MM, Pazicni S, Andrews AJ, Penner-Hahn JE, Al-Hashimi HM, Fierke CA: **NMR and XAS reveal an inner-sphere metal binding site in the P4 helix of the metallo-ribozyme ribonuclease P**. *Proc Natl Acad Sci USA* 2010, **107**:2479-2484.

85. Christian EL, Anderson VE, Carey PR, Harris ME: **A quantitative Raman spectroscopic signal for metal-phosphodiester interactions in solution**. *Biochemistry* 2010, **49**:2869-2879.

86. •• Roh JH, Tyagi M, Briber RM, Woodson SA, Sokolov AP: **The dynamics of unfolded versus folded tRNA: the role of electrostatic interactions**. *J Am Chem Soc* 2011, **133**:16406-16409.
Contrary to conventional interpretations, Mg^{2+} increases local dynamics of tRNA by changing the electrostatic environment.

87. •• Tan ZJ, Chen SJ: **Predicting ion binding properties for RNA tertiary structures**. *Biophys J* 2010, **99**:1565-1576.
The authors are developing an all-atom model to predict the ion electrostatics in RNA folding. This new model can treat ion correlation and fluctuation effects for atomistic RNA structures.

88. Tan ZJ, Chen SJ: **Predicting electrostatic forces in RNA folding**. *Methods Enzymol* 2009, **469**:465-487.